中国科学院高能物理研究所
Institute of High Energy Physics
Chinese Academy of Sciences

ATLAS EXPERIMENT

Searches for strong production of supersymmetric particles

Jiarong Yuan
on behalf of the ATLAS Collaboration

EPS-HEP 2025
Marseille
7th, July, 2025

Supersymmetry (SUSY)

Phys. Rep. 1116 (2025) 261-300
ATL-PHYS-PUB-2024-014

- Some limitations of the Standard Model of particle physics:
  - Dark matter
  - Hierarchy problem
  - Unification of the forces
- SUSY is one of the most appealing BSM theories
  - Strong SUSY: higher cross-section; energetic jets
  - Squark $\tilde{q}$, gluino $\tilde{g}$
- Strong SUSY searches
  - Many jets (light and b-/c-tag)
  - Possibility of many leptons
  - Large missing transverse momentum (E_T^{miss}, MET)

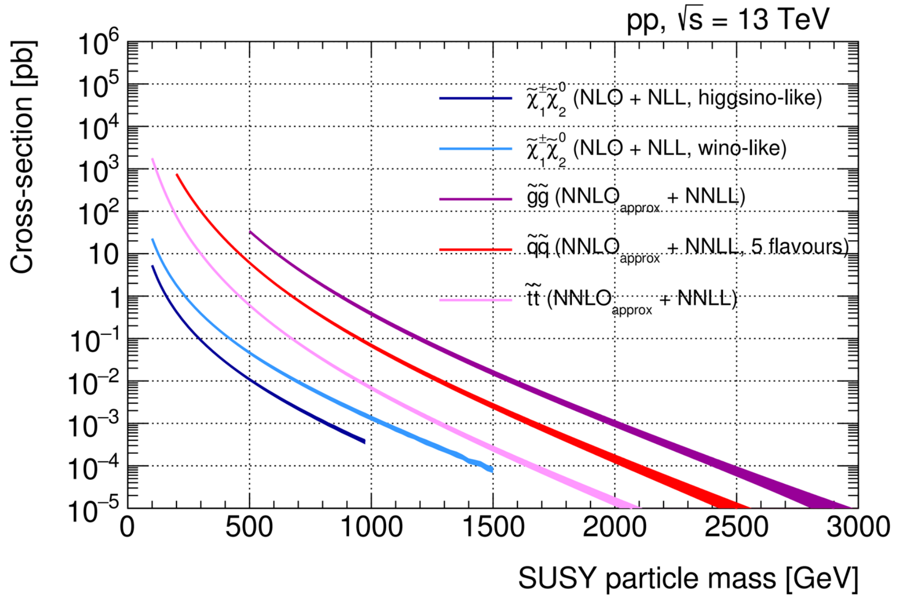

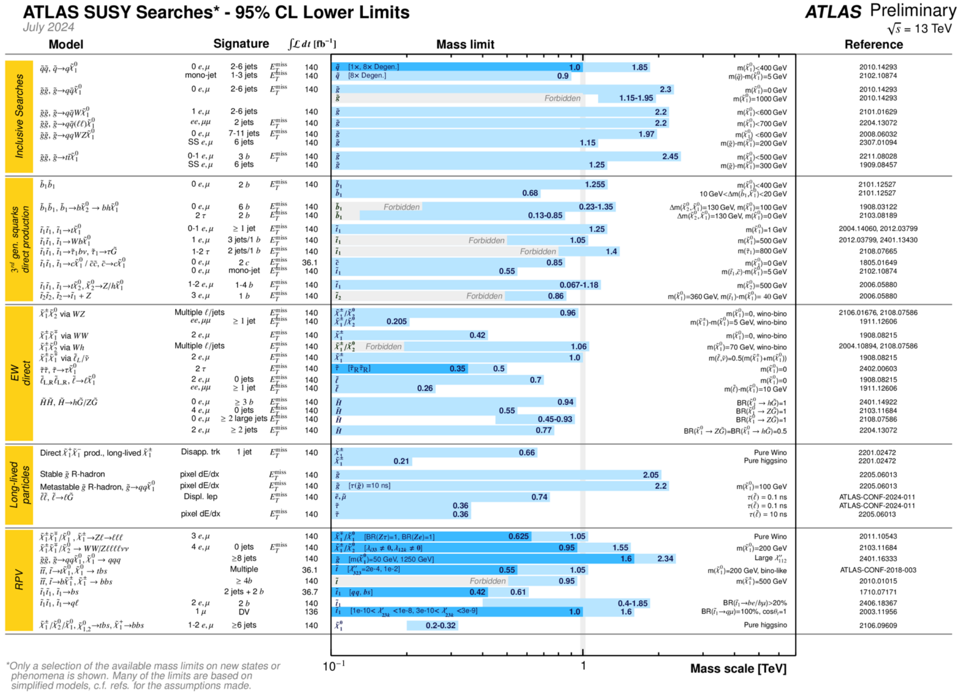

Latest results from ATLAS in strong SUSY production

- **JHEP 03 (2024) 139**
  Search for new phenomena with top-quark pairs and large missing transverse momentum
- **JHEP 02 (2025) 193** NEW
  Search for supersymmetry in final states with missing transverse momentum and charm-tagged jets NEW
- **ATL-PHYS-PUB-2025-010**
  Reinterpretation of searches for flavour-violating supersymmetry into flavour-violating dark matter models

- Full Run-2 dataset
- Exclusion limits reach up to ~2.5 TeV for $\tilde{g}$ and ~2 TeV for 1st, 2nd generation $\tilde{q}$
- Exclusion up to 1.3 TeV in $\tilde{b}_1$ mass and 1.2 TeV in $\tilde{t}_1$ mass

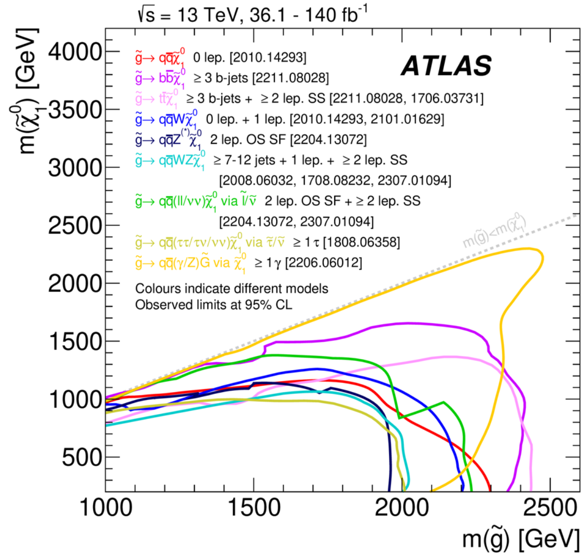

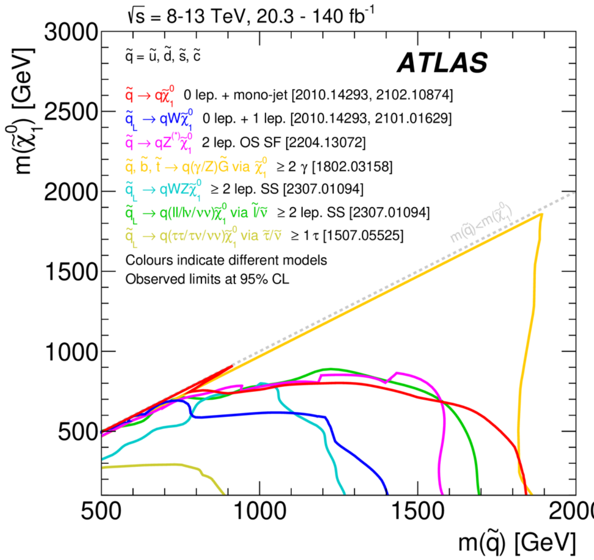

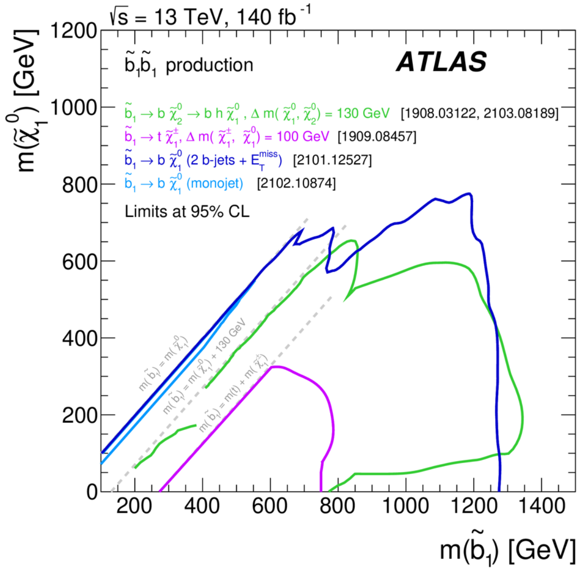

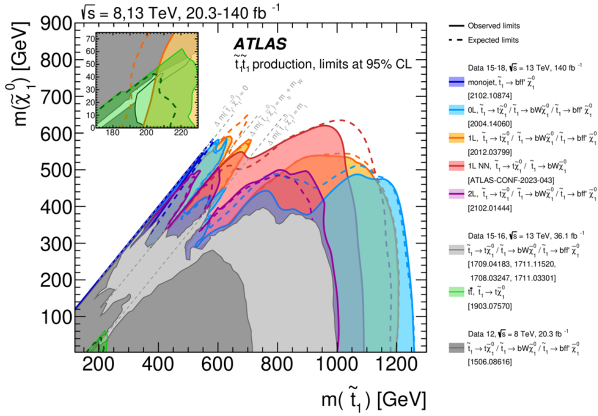

Phys. Rep. 1116 (2025) 261-300
SearchesPublicResults

Stop to top 1L: Introduction

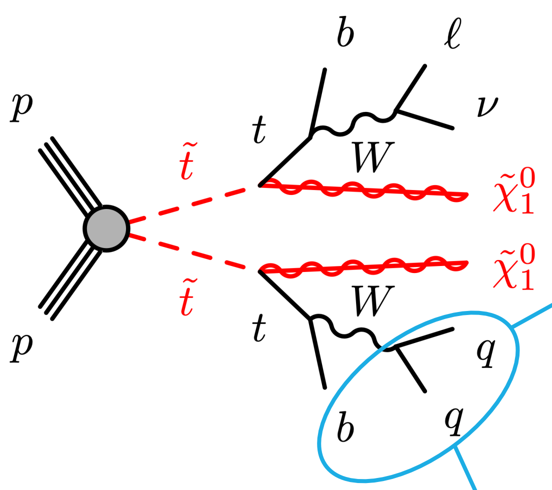

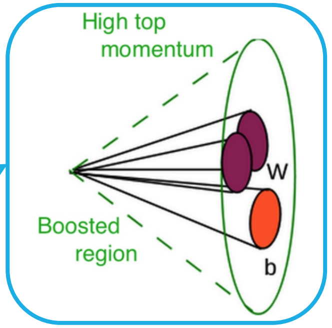

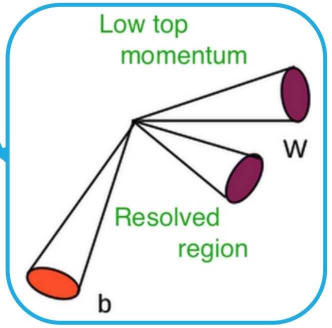

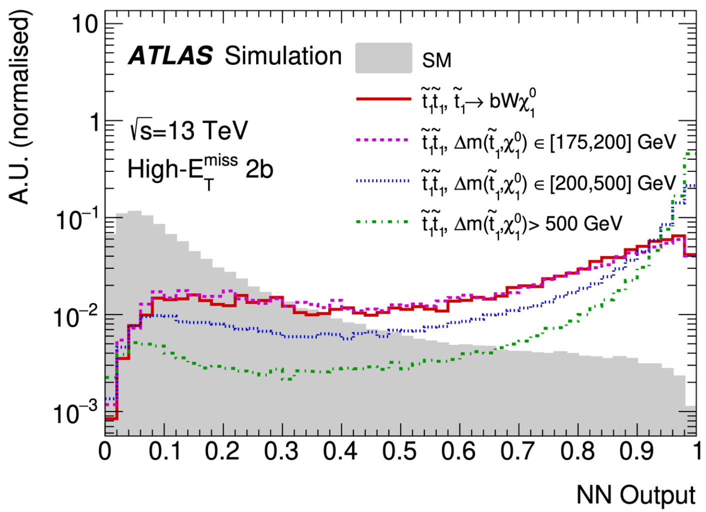

For each region, one NN event classifier (stop-NN) is trained using all signal models. Each region is split into CR, VR, SR by NN selection

Final state: 1L + large-R t-jet, b-jets + high E_T^{miss}

- **Boosted**
- $\geq$ 1 large-R jet ($p_T > 600$ GeV)
- Multivariate classifier to identify top jets
- 80% top-tagging efficiency
- Six orthogonal regions: top-tagging, b-number and bt overlap

- **Resolved (High-E_T^{miss})**
- 0 large-R jet ($p_T > 600$ GeV)
- Top-NN to reconstruct the hadronic top using 2-3 jet combinations with 1 b-jet
- 70% selection efficiency ($p_T \in [200,600]$ GeV)
- Two orthogonal regions: 1 or $\geq$ 2 b-jet

Large-R jets: anti-k_t $R = 1.0$

JHEP 03 (2024) 139

Stop to top 1L: Background Estimation

- Dominant backgrounds: $t\bar{t}$ ($t\bar{t}$-$1L$, $t\bar{t}$-$2L$), single-top, W +jets
- Dedicated CRs: binned in $m_T \times q(\ell)$
  - Different behaviors of $t\bar{t}$ ($t\bar{t}$-$1L$, $t\bar{t}$-$2L$) and W +jets
  - Estimated simultaneously.

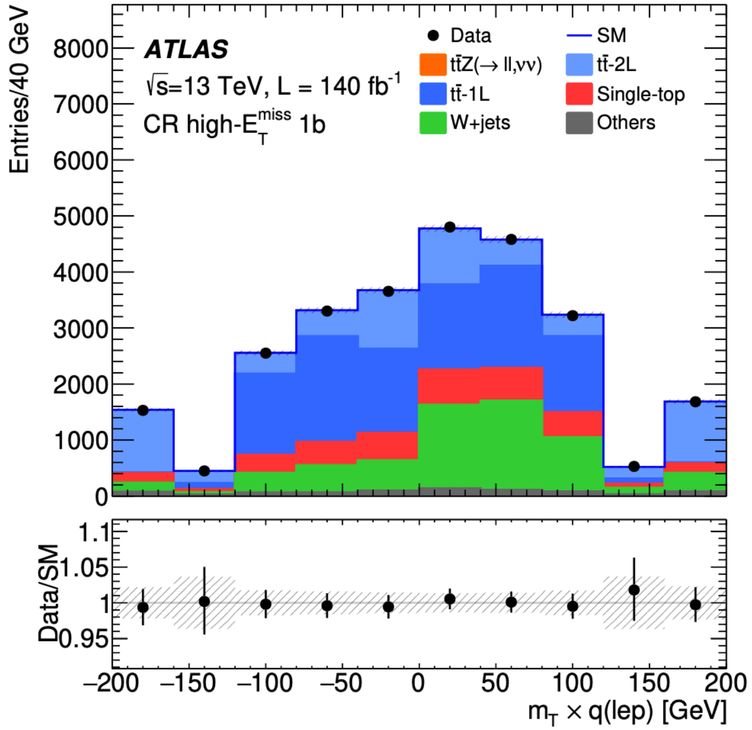

- $ttZ(\rightarrow \nu\bar{\nu})$
  - Signal-like kinematic signature, but small cross-section
  - Only validation
  - Three-lepton VRs for $ttZ(\rightarrow \ell\bar{\ell})$
    - Two same-flavor-opposite-sign leptons with a $Z \rightarrow \ell\ell$ selection
    - Recalculate MET with the two leptons subtracted

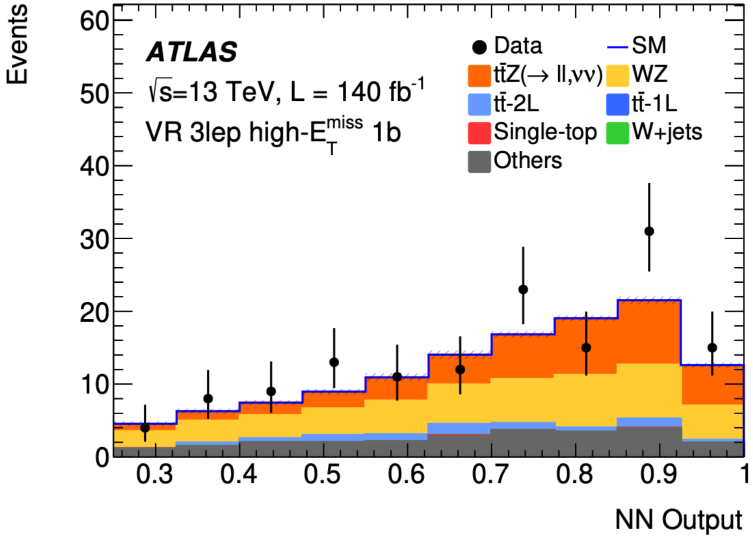

Stop to top 1L: Results

- No significant excess above the SM
- Set exclusion limits

- Exclusion limits compared with previous 1L results
- Cover the valley between bulk and compressed regions

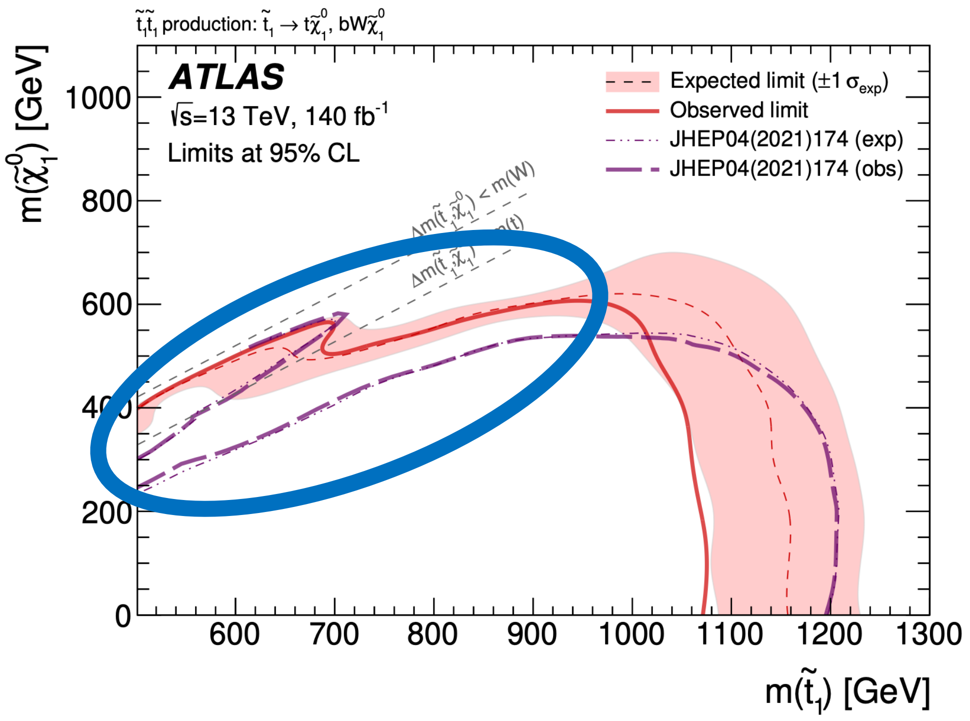

- Combination with stop 0L results
- Improve the sensitivity at compressed region
- For a massless LSP, exclusion up to ~1.2 TeV

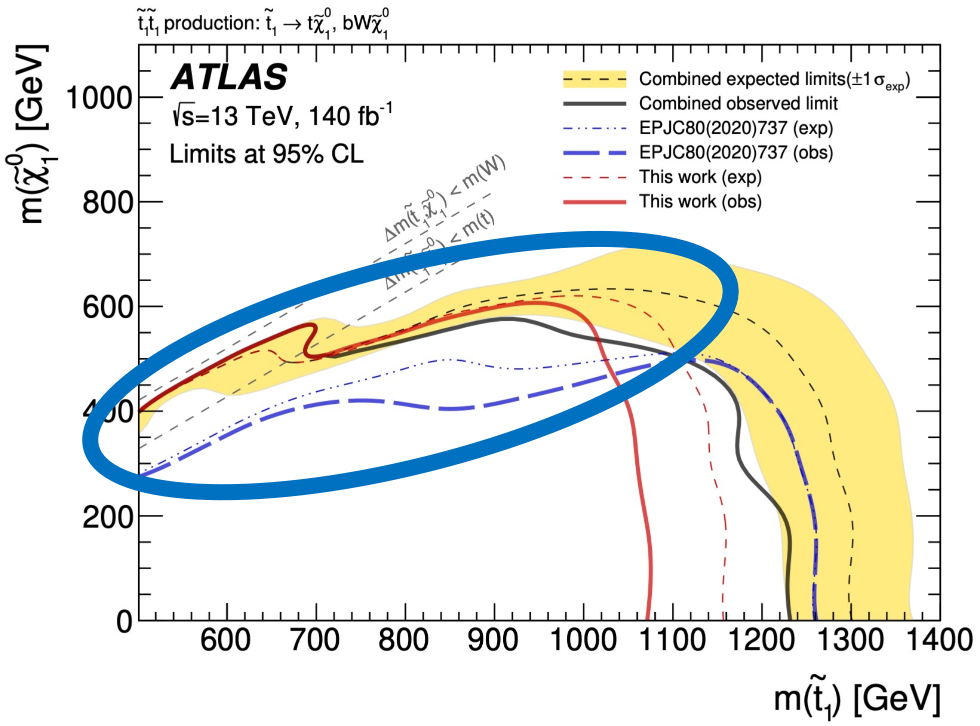

JHEP 03 (2024) 139

SUSY cc and E_T^{miss}: Introduction

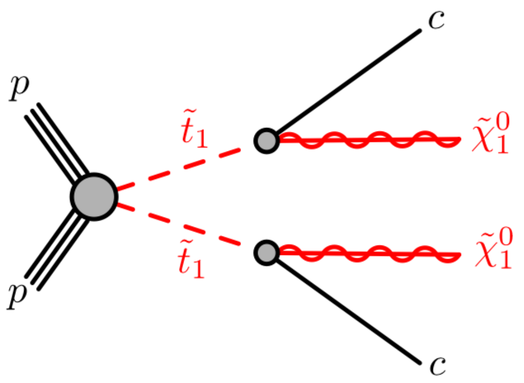

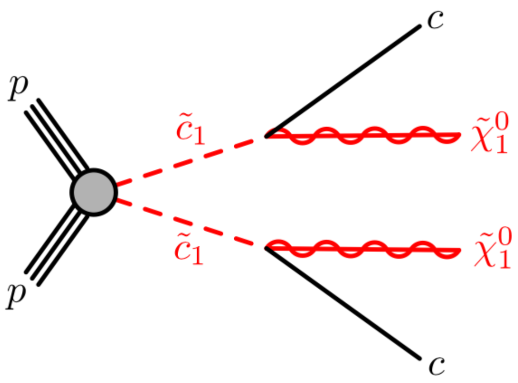

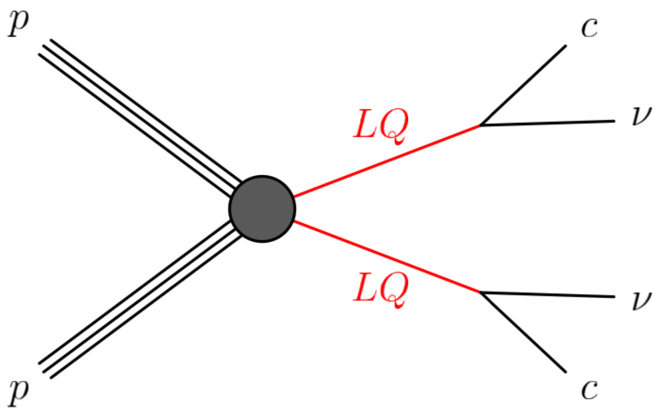

minimal flavour violation for most SUSY analyses
Additional flavour violation allows $\tilde{t}_1 \to c\tilde{\chi}_1^0$

Vector LQ: $\mathcal{B}(LQ \to c\nu_\tau) = 0.5$
Scalar LQ: $\mathcal{B}(LQ \to c\nu_{e/\mu}) \in [0,1]$

- Dedicated c-tagging algorithm: $\mathrm{DL1r_c}$
  - 20% selection efficiency (with b-veto)
- Two orthogonal categories:
  - High Mass regions: high $\boldsymbol{E_T^{miss}}$ significance, energetic c-jets
  - Compressed regions: high-p_T ISR jets boost sparticles, **Recursive Jigsaw Reconstruction (boost topology)**

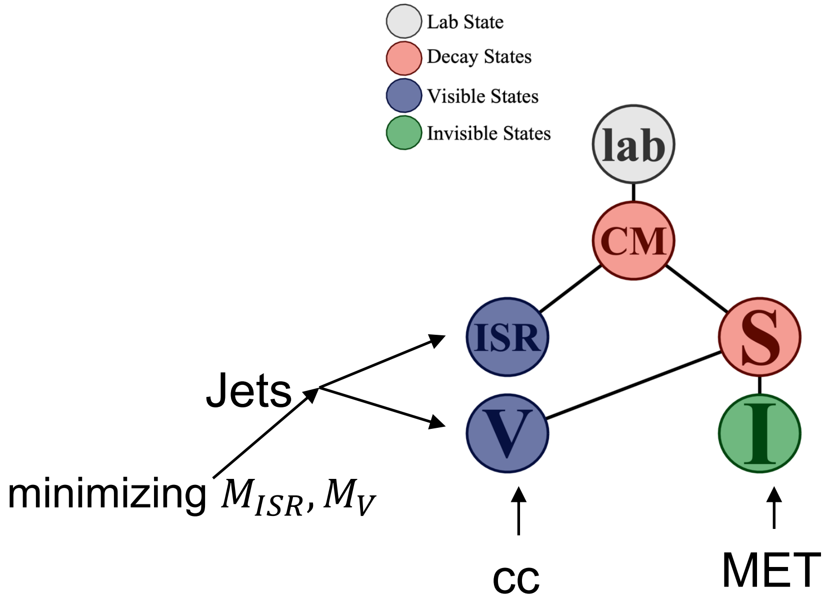

JHEP 02 (2025) 193
DL1r: Eur. Phys. J. C 83 (2023) 681

SUSY cc and E_T^{miss}: Background Estimation

- Dominant backgrounds: $Z + \text{jets}$, $W + \text{jets}$
- Z CR (2L): $\ell\ell$ are treated as invisible as a proxy for neutrinos for MET and all the other variables

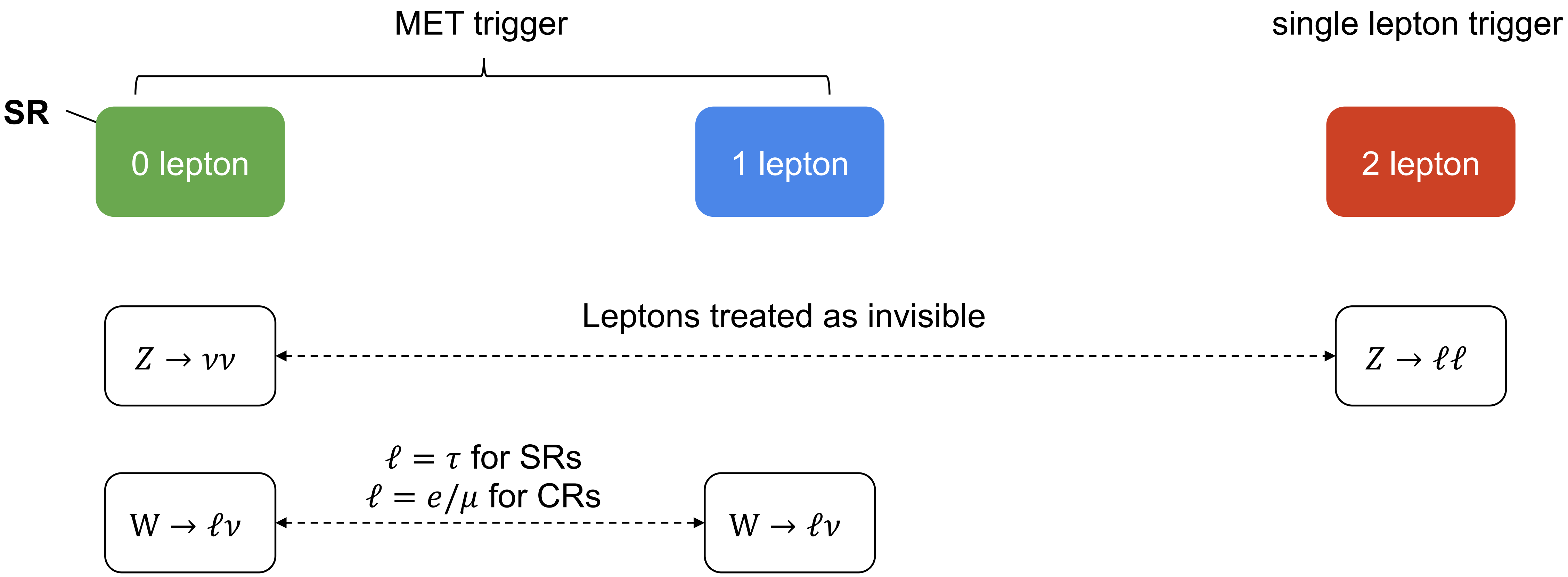

SUSY cc and E_T^{miss}: Results

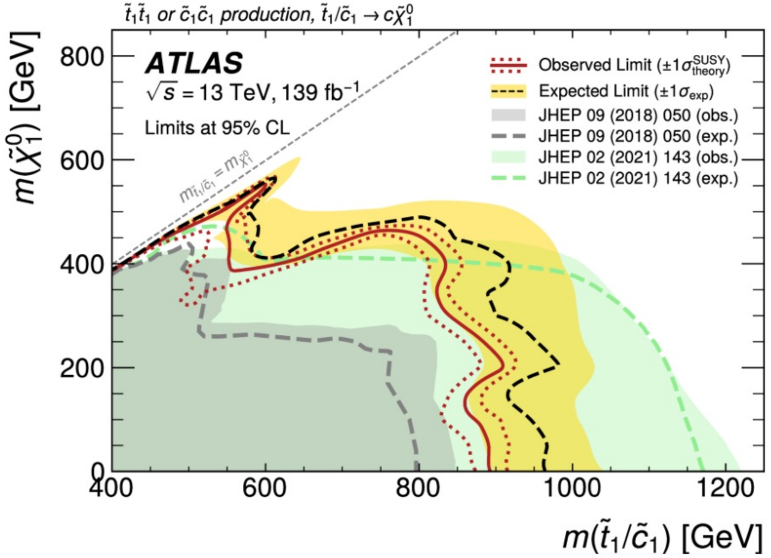

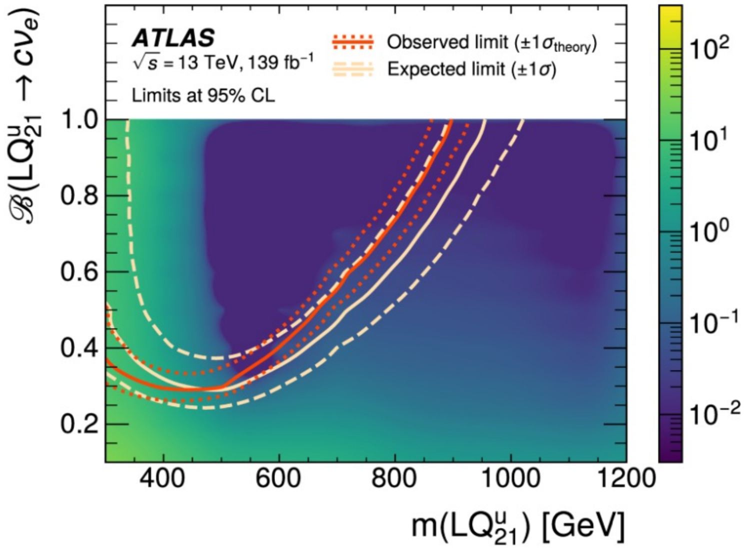

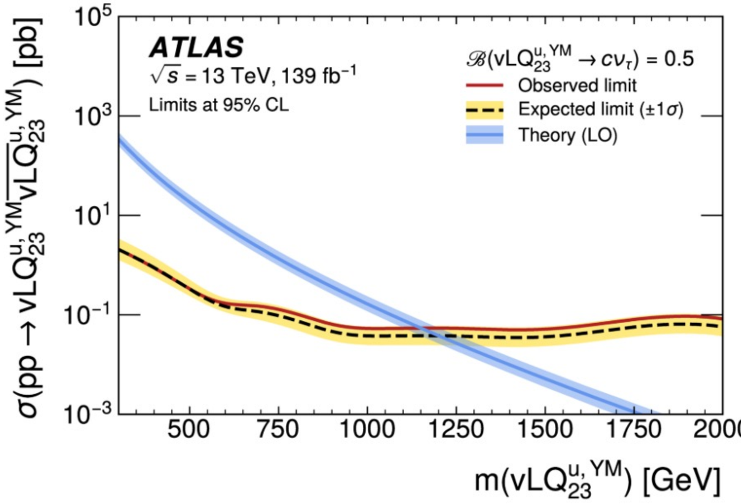

- No significant excess over the SM
- Limits in squark models reach up to 900 GeV
  - Improve ~50 GeV wrt previous result (grey)
  - Better results at compressed region wrt single-squark-production limit w/o c-tagging (green)
- Limits in scalar (vector) LQ models reach up to 900 (1150) GeV

JHEP 02 (2025) 193

Reinterpretation for DM: Signal Model

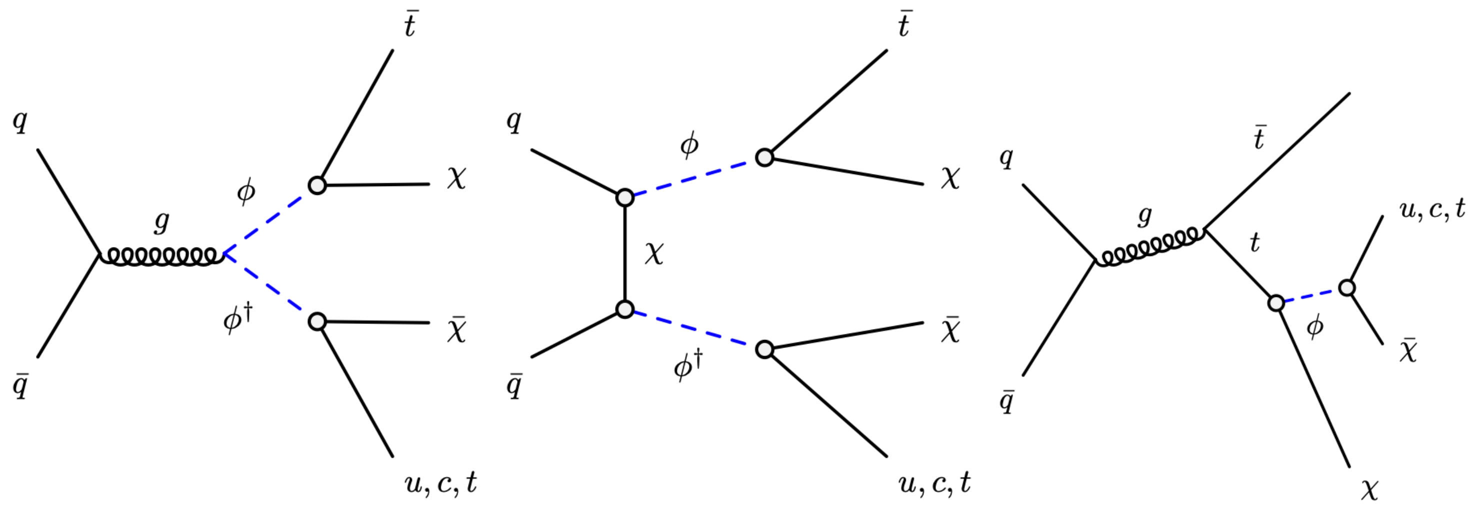

- Dark Minimal Flavour violation
  - DM flavours χ_i $(i = 1,2,3)$ couple with the SM quark via a mediator ϕ
  - The coupling is a source of flavour violation

$$\phi \rightarrow \chi q, q = u, c, t$$

- Four benchmark scenarios
  - LH/RH, DM mass, coupling strength, and mixing angles
- Reinterpreted analysis: SUSY tc+E_T^{miss}

Benchmark	m_χ	Couplings	Mixing angles
$D_{\lambda,11} = D_{\lambda,22}$; $\theta_{12} = \theta_{23} = 0$; $\delta_{ij} = 0$			
RH-SFF	200 GeV	$D_{\lambda,33} = D_{\lambda,11} + 1.0$	$\sin\theta_{13} = 0.25$
RH-QDF	150 GeV	$D_{\lambda,33} = D_{\lambda,11} + 0.2$	$\sin\theta_{13} = 0.2$
LH-QDF1	150 GeV	$D_{\lambda,33} = D_{\lambda,11} + 0.1$	$\sin\theta_{13} = 0.1$
LH-QDF2	450 GeV	$D_{\lambda,33} = D_{\lambda,11} + 0.2$	$\sin\theta_{13} = 0.2$
Parameters to scan: m_ϕ and $D_{\lambda,11}$			

ATL-PHYS-PUB-2025-010

tc+E_T^{miss} JHEP 07(2024)250

Reinterpretation for DM: Selection

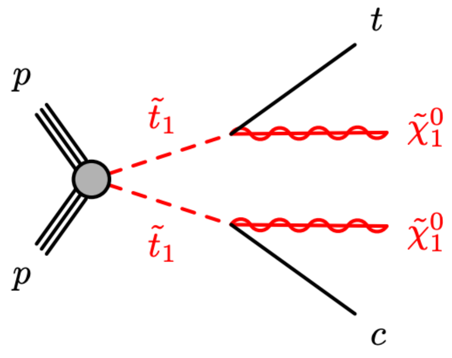

- Final state: top + c + MET
- B-tag using $\mathrm{DL1r}$, c-tag using $\mathrm{DL1r_c}$ (the same tagger used in cc $+E_T^{miss}$ analysis)
- DNN top tagger for large-R jets (the same tagger used in stop 1L analysis)
- 0 L
- Four orthogonal SRs for different phase space

Bulk
Boosted
SRA

- ≥ 1 large-R top-jet
- Leading c- or b-jet
- $m_{T2} \geq 450$ GeV

Intermediate

SRC
Boosted

- ≥ 1 large-R top-jet
- Leading c- or b-jet
- $m_{T2} \in [200, 450]$ GeV

SRB
Resolved

- 0 large-R top-jet
- Leading c- or b-jet

Compressed
SRD

- Leading light jet (ISR)
- NN to separate signal from background

ATL-PHYS-PUB-2025-010
tc+E_T^{miss} JHEP 07(2024)250

Reinterpretation for DM: Background Estimation

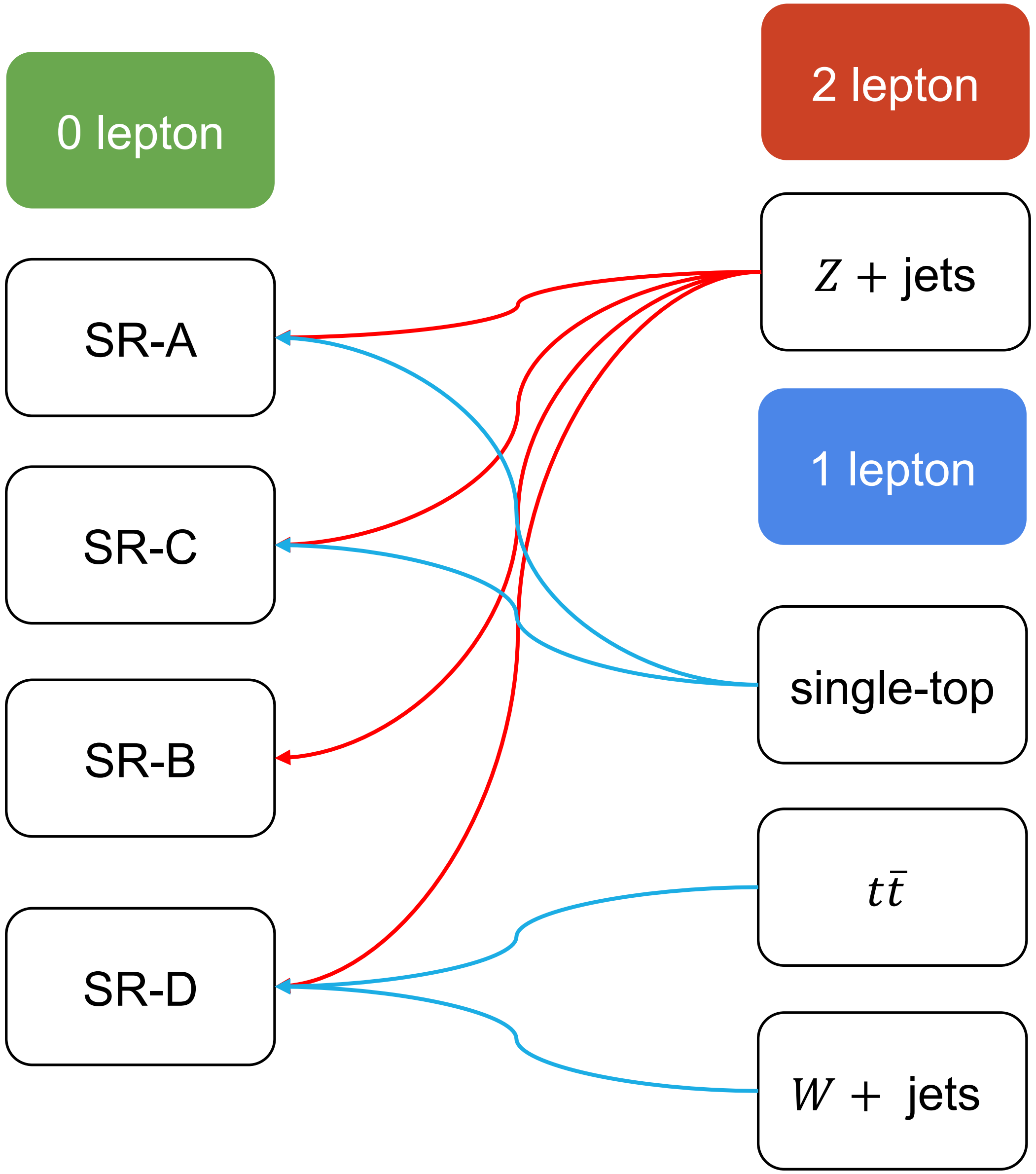

- Z + jets CRs
  - Two leptons are subtracted from MET to mimic neutrinos in SR
- $t\bar{t}$, W + jets CRs
  - Treat the lepton as a jet to mimic a hadronic τ in SR
- Orthogonal to SR via lepton requirement

ATL-PHYS-PUB-2025-010

tc+E_T^{miss} JHEP 07(2024)250

Reinterpretation for DM: Results

- No significant excess over SM
- Set limits on new mediator mass and its coupling strength
- **First constraints for Dark Minimal Flavour violation models at LHC**
- If DM mass is around 150 to 200 GeV, the exclusion limits can reach up to 1.2 TeV for $D_{\lambda,11} \approx 2$
    - Weaker sensitivity with $D_{\lambda,11} \leq 1$
- With a high DM mass assumed around 450 GeV, mediator mass can exclude $[750, 1100]$ GeV for $D_{\lambda,11} \geq 1.5$

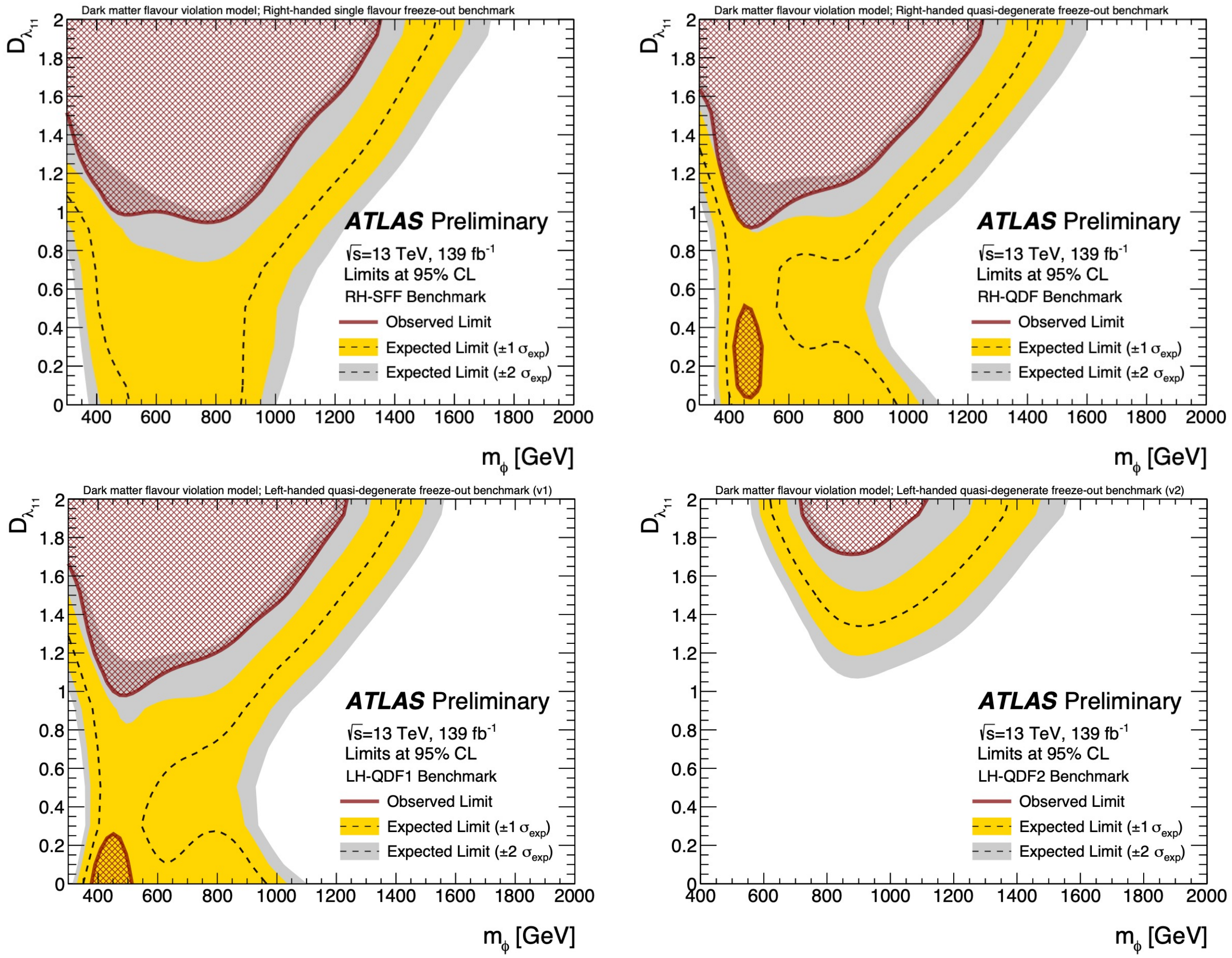

Conclusion

- Three recent results using full Run2 dataset presented
  - Strong production of stop pair with top-pair
  - Strong production of top/charm squark with charm-jets
  - Interpretation of LQ, DM
- No significant excess over SM. Exclusion limits for:
  - Top squark mass and branching ratios
  - Charm squark mass
  - LQ and DM models
- Many Run 2 results already public from ATLAS Collaboration!
- Many new Run 3 analyses in the works!

- SearchesPublicResults
- JHEP 03 (2024) 139
- JHEP 02 (2025) 193
- ATL-PHYS-PUB-2025-010

BACKUP

Stop to top 1L

Analysis Category	High-$E_{\mathrm{T}}^{\mathrm{miss}}$ 1b	High-$E_{\mathrm{T}}^{\mathrm{miss}}$ 2b	Boosted 1b-lep-0t	Boosted 1b-had-0t	Boosted 2b-0t	Boosted 1b-lep-1t	Boosted 1b-had-1t	Boosted 2b-1t
N(lR jet, $p_{\mathrm{T}} > 600$ GeV)	0		≥ 1					
N(top-tagged lR jet)	-		0			≥ 1		
$N_{b-\mathrm{jet}}$ with $\Delta R(b, lR\text{ jet}) < 1.1$	-		0	≥ 1	≥ 1	0	≥ 1	≥ 1
$N_{b-\mathrm{jet}}$ with $\Delta R(b, lR\text{ jet}) > 1.1$	-		≥ 1	0	≥ 1	≥ 1	0	≥ 1
top-NN-tagged multiplet	✓		-					
$N_{b-\mathrm{jet}}$	1	≥ 2	-					
$N_{\mathrm{light-jet}}$	≥ 2	≥ 1	-					
$\mathrm{top_{had}}$ candidate	top-NN multiplet		lR jet					
$\mathrm{top_{lep}}$ candidate	$\ell + \mathrm{j}$	$\ell + b$	$\ell + b$	$\ell(+\mathrm{j})$	$\ell + b$	$\ell + b$	$\ell(+\mathrm{j})$	$\ell + b$
Event NN selection	See table 3							

Table 2. Summary of the selections for each event category together with the definitions of the hadronic and leptonic top quark candidates. Trigger, lepton and $E_{\mathrm{T}}^{\mathrm{miss}}$ selections are described in the text. Large-R jets are referred to as 'lR' for brevity.

Category	stop-NN CR Range	stop-NN VR Range	stop-NN SR Range	Eff.
High-$E_{\mathrm{T}}^{\mathrm{miss}}$ 1b	$[0.2, 0.64)$	$[0.64, 0.79)$	$[0.79, 1.0]$	0.4-0.9
High-$E_{\mathrm{T}}^{\mathrm{miss}}$ 2b	$[0.1, 0.56)$	$[0.56, 0.70)$	$[0.70, 1.0]$	0.5-0.9
Boosted 1b-lep-1t	$[0.0, 0.65)$	$[0.65, 0.80)$	$[0.80, 1.0]$	0.5-0.9
Boosted 1b-had-1t	$[0.0, 0.65)$	$[0.65, 0.85)$	$[0.85, 1.0]$	0.6-0.9
Boosted 2b-1t	$[0.0, 0.75)$	$[0.75, 0.95)$	$[0.95, 1.0]$	0.6-0.8
Boosted 1b-lep-0t	$[0.0, 0.70)$	$[0.70, 0.85)$	$[0.85, 1.0]$	0.6-0.8
Boosted 1b-had-0t	$[0.0, 0.75)$	$[0.75, 0.95)$	$[0.95, 1.0]$	0.4-0.8
Boosted 2b-0t	$[0.0, 0.65)$	$[0.65, 0.80)$	$[0.80, 1.0]$	0.6-0.9

Category	Fitted observable CR	Fitted observable SR	$\mathrm{NF}_{\mathrm{top-1L}}^{\mathrm{High-met}}$	$\mathrm{NF}_{\mathrm{top-1L}}^{\mathrm{Boosted}}$	$\mathrm{NF}_{\mathrm{top-2L}}^{\mathrm{High-met}}$	$\mathrm{NF}_{\mathrm{top-2L}}^{\mathrm{Boosted}}$	$\mathrm{NF}_{W}^{\mathrm{High-met}}$	$\mathrm{NF}_{W}^{\mathrm{Boosted}}$	$\mathrm{NF}_{\mathrm{singletop}}$
High-$E_{\mathrm{T}}^{\mathrm{miss}}$ 1b	$m_{\mathrm{T}} \times q(\ell)$	NN	✓		✓		✓		✓
High-$E_{\mathrm{T}}^{\mathrm{miss}}$ 2b	$m_{\mathrm{T}} \times q(\ell)$	NN	✓		✓		✓		✓
Boosted 1b-lep-1t	$m_{\mathrm{T}} \times q(\ell)$	NN		✓		✓		✓	✓
Boosted 1b-had-1t	$m_{\mathrm{T}} \times q(\ell)$	NN		✓		✓		✓	✓
Boosted 2b-1t	$m_{\mathrm{T}} \times q(\ell)$ (low-m_{T2}) Yield (high-m_{T2})	NN		✓		✓		✓	✓
Boosted 1b-lep-0t	$m_{\mathrm{T}} \times q(\ell)$	NN		✓		✓		✓	✓
Boosted 1b-had-0t	$m_{\mathrm{T}} \times q(\ell)$	NN		✓		✓		✓	✓
Boosted 2b-0t	$m_{\mathrm{T}} \times q(\ell)$ (low-m_{T2}) Yield (high-m_{T2})	NN		✓		✓		✓	✓

Stop to top 1L

	$\tilde{t}_1\tilde{t}_1$, $m(\tilde{t}_1, \tilde{\chi}_1^0)$ GeV		$t\bar{t}$+DM, $m(a,\chi)$ GeV	
	$(1000, 600)$	$(1200, 200)$	$(50, 1)$	$(150, 1)$
$\mu \pm \sigma(\mu)$ (total uncertainty)	$0.25^{+0.42}_{-0.25}$	$0.8^{+0.7}_{-0.5}$	$0.08^{+0.10}_{-0.08}$	$0.12^{+0.13}_{-0.12}$
Data statistical uncertainty	82 %	74 %	67 %	69 %
Background modelling	45 %	62 %	51 %	48 %
MC statistical uncertainty	25 %	20 %	34 %	33 %
Jet energy scale and resolution	20 %	13 %	29 %	28 %
Flavour tagging efficiency	18 %	10 %	21 %	21 %

with unity within uncertainties. The NFs for the $t\bar{t}$-1L (-2L) background are 1.02 ± 0.06 (1.09 ± 0.05) and 1.07 ± 0.06 (1.29 ± 0.13) in the high-$E_{\mathrm{T}}^{\mathrm{miss}}$ and boosted regions, respectively. The NFs for the W+jets backgrounds are 1.30 ± 0.15 and 1.33 ± 0.11 in the same regions. The single-top NF is 1.4 ± 0.4, with the large uncertainty due in part to the correlation with the uncertainty related to the removal of the on-shell tW contributions. Similar values are

Wilson coefficient	Observed (Expected) upper limit on $\sqrt{\lvert V_{ij}\rvert}/\Lambda$ [TeV^{-1}]	Observed (Expected) lower limit on Λ for $\lvert V_{ij}\rvert = 4\pi$ [TeV]
$V_{LL} > 0$	1.59 $(1.44^{1.58}_{1.31})$	2.23 $(2.47^{2.71}_{2.25})$
$m_{\nu\bar{\nu}} < 1$ TeV	1.84 $(1.66^{1.82}_{1.51})$	1.93 $(2.14^{2.35}_{1.95})$
$m_{\nu\bar{\nu}} < 2$ TeV	1.62 $(1.46^{1.61}_{1.36})$	2.18 $(2.42^{2.66}_{2.21})$
$V_{LL} < 0$	1.66 $(1.52^{1.66}_{1.40})$	2.13 $(2.33^{2.53}_{2.14})$
$m_{\nu\bar{\nu}} < 1$ TeV	1.96 $(1.80^{1.95}_{1.66})$	1.81 $(1.97^{2.13}_{1.82})$
$m_{\nu\bar{\nu}} < 2$ TeV	1.70 $(1.56^{1.69}_{1.44})$	2.08 $(2.28^{2.47}_{2.10})$
$V_{LR} > 0$	1.67 $(1.53^{1.66}_{1.40})$	2.12 $(2.32^{2.53}_{2.13})$
$m_{\nu\bar{\nu}} < 1$ TeV	1.92 $(1.78^{1.94}_{1.64})$	1.84 $(1.99^{2.16}_{1.82})$
$m_{\nu\bar{\nu}} < 2$ TeV	1.70 $(1.56^{1.70}_{1.44})$	2.08 $(2.27^{2.47}_{2.08})$
$V_{LR} < 0$	1.63 $(1.49^{1.63}_{1.36})$	2.17 $(2.38^{2.60}_{2.18})$
$m_{\nu\bar{\nu}} < 1$ TeV	1.86 $(1.72^{1.89}_{1.58})$	1.91 $(2.06^{2.25}_{1.88})$
$m_{\nu\bar{\nu}} < 2$ TeV	1.66 $(1.52^{1.67}_{1.40})$	2.13 $(2.33^{2.54}_{2.13})$

SUSY cc and E_T^{miss}

Variable	SR-HM1	SR-HM2	SR-HM3	SR-HM-Disc
Number of leptons	$= 0$			
Jet p_{T} [GeV]	> 40			
Number of b-tagged jets	$= 0$			
$p_{\mathrm{T}}(j_1)$ [GeV]	> 250			
$\Delta\phi(\vec{p}_{\mathrm{T}}^{\mathrm{miss}}, \vec{p}_{\mathrm{T}}(j_4))$	> 0.4			
Number of c-tagged jets	≥ 2			
Leading jet is c-tagged	yes			
$m_{\mathrm{T}}^{\mathrm{min}}(c)$ [GeV]	> 300			
$p_{\mathrm{T}}(j_2)$ [GeV]	> 200	> 150		
m_{cc} [GeV]	> 200	$200-400$	$400-600$	> 200
$E_{\mathrm{T}}^{\mathrm{miss}}$ Sig.	> 22	$15-22$		> 15

Variable	SR-Comp1	SR-Comp2	SR-Comp3	SR-Comp-1c
Number of leptons	$= 0$			
Jet p_{T} [GeV]	> 20			
Number of b-tagged jets	$= 0$			
$p_{\mathrm{T}}(j_1)$ [GeV]	> 250			
$\Delta\phi(\vec{p}_{\mathrm{T}}^{\mathrm{miss}}, \vec{p}_{\mathrm{T}}(j_4))$	> 0.4			
Number of c-tagged jets	≥ 2			$= 1$
Leading jet is c-tagged	no			
$m_{\mathrm{T}}^{\mathrm{min}}(c)$ [GeV]	—	> 80	> 120	< 250
m_{cc} [GeV]	—		> 100	—
$p_{\mathrm{T}}^{\mathrm{CM}}$ [GeV]	—			< 10
m_{V} [GeV]	—			< 80
$\Delta\phi(\vec{p}_{\mathrm{T}}^{\mathrm{miss}}, j_1)$	—			> 2
$N_{c\text{-jets}}^{\mathrm{S}}$	≥ 2			$= 1$
$p_{\mathrm{T}}^{\mathrm{ISR}}$ [GeV]	> 550	> 500	> 400	> 700
R_{ISR}	> 0.85	$0.75-0.85$	> 0.65	$0.9-1.0$

$\mathrm{DL1r_c}$ tagger constructed from DL1r

$$\mathrm{DL1r_c} = \log\left(\frac{p_c}{f_b p_b + (1-f_b) p_u}\right)$$

SUSY cc and E_T^{miss}

Variable	CRZ-HM	CRZ-Comp	CRZ-Comp-1c
Used for	SR-HM	SR-Comp	SR-Comp-1c
$p_{\mathrm{T}}(j_1)$	> 250 GeV		> 350 GeV
Number of c-tagged jets	≥ 2		$= 1$
Leading jet is c-tagged	yes	no	
Number of signal muons/electrons	$= 2$		
Passed single-electron/muon triggers	yes		
$p_{\mathrm{T}}(\ell_1)$ [GeV]	> 30		
$m_{\ell\ell}$ [GeV]	76−106		
$E_{\mathrm{T}}^{\mathrm{miss}}$ [GeV]	< 200		
$E_{\mathrm{T}}^{\mathrm{miss}\prime}$ [GeV]	> 200		
m_{cc} [GeV]	> 150	—	
$m_{\mathrm{T}}^{\mathrm{min}\prime}(c)$ [GeV]	> 150	—	< 250
$E_{\mathrm{T}}^{\mathrm{miss}\prime}$ Sig.	> 10	—	
$N_{c\text{-jets}}^{\mathrm{S}\prime}$	—	≥ 1	$= 1$
$R_{\mathrm{ISR}}^{\prime}$	—	> 0.75	0.9−1.0
$p_{\mathrm{T}}^{\mathrm{ISR}\prime}$ [GeV]	—		> 550
$\Delta\phi(\vec{p}_{\mathrm{T}}^{\mathrm{miss}\prime}, j_1)$	—		> 2

Variable	CRW-HM	CRW-Comp	CRW-Comp-1c
Used for	SR-HM	SR-Comp	SR-Comp-1c
$p_{\mathrm{T}}(j_1)$ [GeV]	> 250		> 350
Number of c-tagged jets	≥ 2		$= 1$
Number of signal muons/electrons	$= 1$		
Passed $E_{\mathrm{T}}^{\mathrm{miss}}$ trigger	yes		
$E_{\mathrm{T}}^{\mathrm{miss}}$ [GeV]	> 250		
m_{cc} [GeV]	> 200	—	
$m_{\mathrm{T}}^{\mathrm{min}}(c)$ [GeV]	> 200	> 120	< 250
$E_{\mathrm{T}}^{\mathrm{miss}}$ Sig.	> 14	—	
Leading jet is c-tagged	yes	no	
$N_{c\text{-jets}}^{\mathrm{S}}$	—	≥ 1	$= 1$
$p_{\mathrm{T}}^{\mathrm{ISR}}$ [GeV]	—	> 400	> 550
R_{ISR}	—	> 0.65	0.9−1.0
τ veto	—	yes	—
$\Delta\phi(\vec{p}_{\mathrm{T}}^{\mathrm{miss}}, j_1)$	—		> 2

Variable	VR-HM	VR-Comp	VR-Comp-1c
Validates backgrounds in	SR-HM	SR-Comp	SR-Comp-1c
Number of c-tagged jets	≥ 2		$= 1$
Passed $E_{\mathrm{T}}^{\mathrm{miss}}$ trigger	yes		
$E_{\mathrm{T}}^{\mathrm{miss}}$ [GeV]	> 250		
m_{cc} [GeV]	> 200	—	
$m_{\mathrm{T}}^{\mathrm{min}}(c)$ [GeV]	> 200	> 80	> 100
Leading jet is c-tagged	yes	no	
$N_{c\text{-jets}}^{\mathrm{S}}$	—	≥ 1	$= 1$
$p_{\mathrm{T}}^{\mathrm{ISR}}$ [GeV]	—	< 400	
R_{ISR}	—	> 0.65	0.85−1.05
τ veto	yes		
$\Delta\phi(\vec{p}_{\mathrm{T}}^{\mathrm{miss}}, j_1)$	—		> 2
$p_{\mathrm{T}}^{\mathrm{CM}}$ [GeV]	—		< 10
m_{V} [GeV]	—		< 80

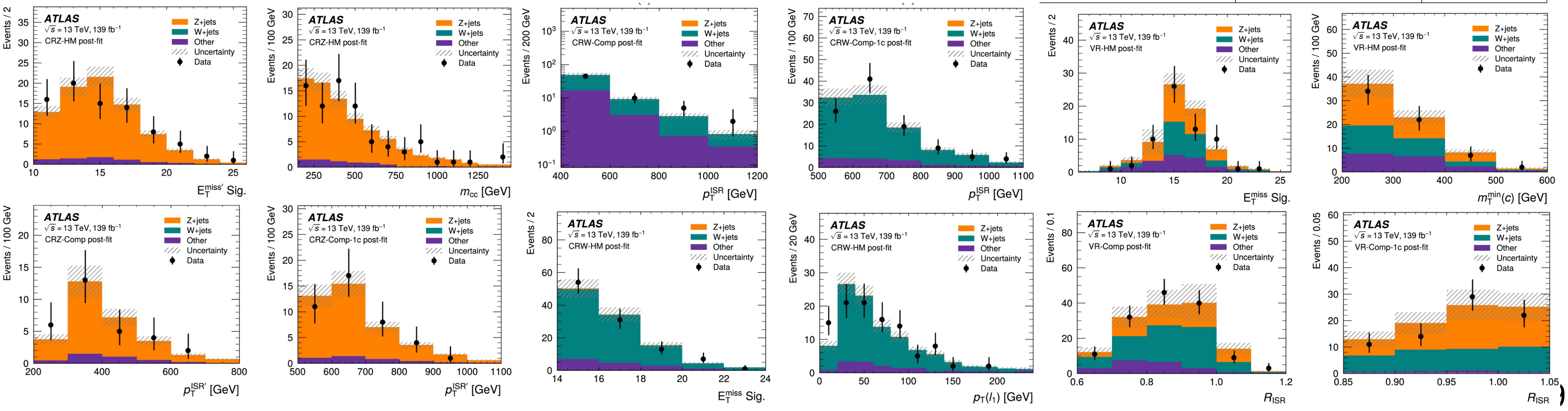

SUSY cc and E_T^{miss}

Region	Normalization factor
HM Z+jets	1.0 ± 0.4
Comp Z+jets	1.0 ± 0.4
Comp-1c Z+jets	1.1 ± 0.4
HM W+jets	1.4 ± 0.6
Comp W+jets	1.3 ± 0.7
Comp-1c W+jets	1.6 ± 0.7

Signal Region	$\langle\epsilon\sigma\rangle_{\rm obs}^{95}$ [fb]	$S_{\rm obs}^{95}$	$S_{\rm exp}^{95}$	$p_{\rm obs}(S=0)$
SR-HM1	0.09	12.8	$9.7^{+4.2}_{-2.9}$	0.19
SR-HM-Disc	0.36	50.7	34^{+13}_{-9}	0.09
SR-Comp3	0.07	9.2	$6.5^{+3.2}_{-2.0}$	0.15
SR-Comp-1c	0.08	11.6	$8.0^{+3.8}_{-2.4}$	0.13

bkg-only fit

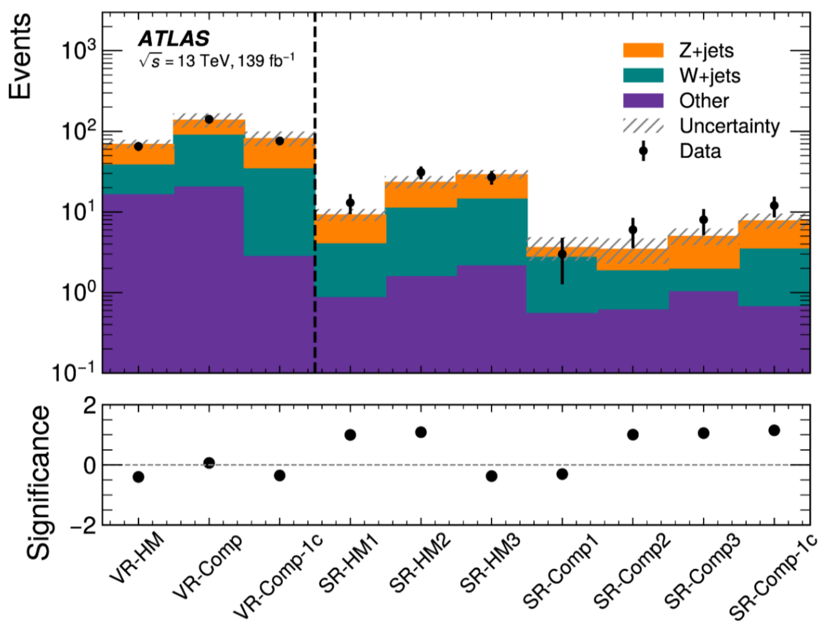

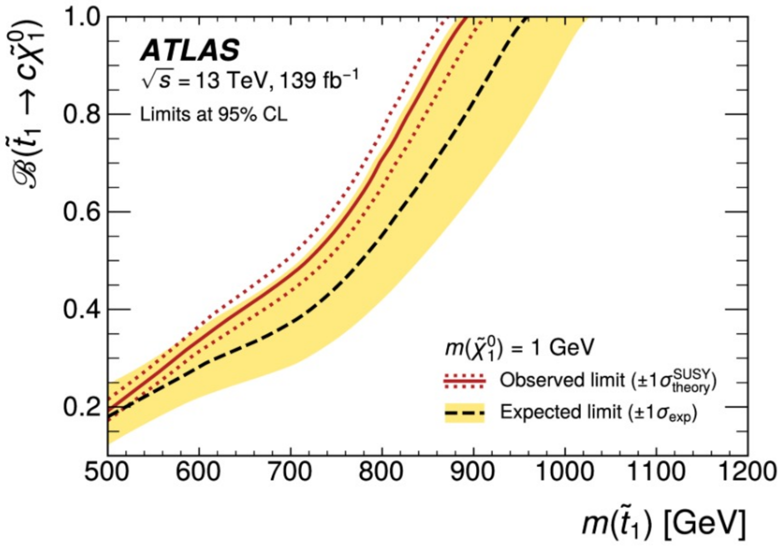

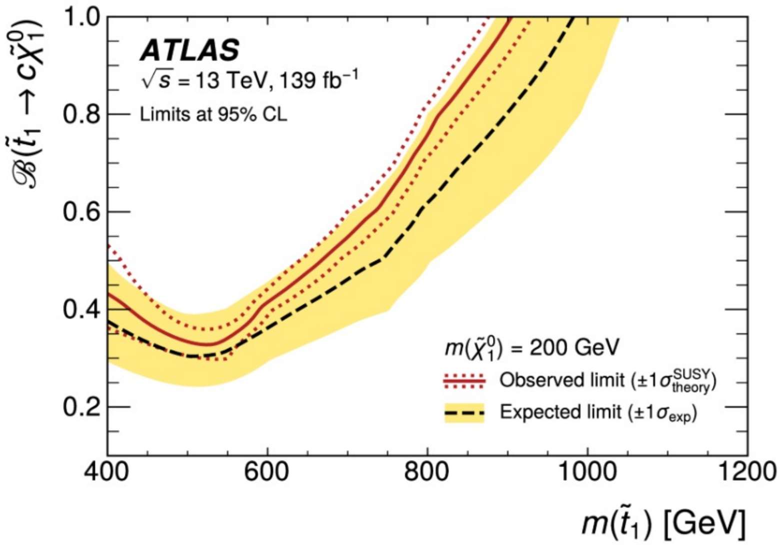

SUSY cc and E_T^{miss}

- R_{ISR}: The projection of the tranverse momentum of the invisible (I) frame in the direction of the ISR frame (Eq. (0.5)). In compressed SUSY signals, an ISR topology boosts the sparticle system such that the neutralinos produced in their decay, which generate the missing transverse momentum in the event, allow for the event to pass the $E_{\mathrm{T}}^{\mathrm{miss}}$ trigger threshold. Because of this, the ISR and sparticle systems tend to be approximately back-to-back in compressed SUSY events, resulting in R_{ISR} values closer to 1, while SM backgrounds tend to populate a wider range of values in R_{ISR}.

- $p_{\mathrm{T}}^{\mathrm{ISR}}$: The total p_{T} of jets in the ISR frame. For SM backgrounds, this is a smoothly falling distribution. For compressed SUSY signals, a high-p_{T} ISR system is required to boost the signal system so that the event passes the $E_{\mathrm{T}}^{\mathrm{miss}}$ trigger threshold. In such cases, a peak at higher $p_{\mathrm{T}}^{\mathrm{ISR}}$ is seen, with the location of the peak typically related to the mass of the parent SUSY particle.

- $N_{c-\mathrm{jets}}^{\mathrm{S}}$: The number of c-tagged jets assigned to the signal (S) frame of the ISR decay tree. For SM processes, RJR tends to assign c-tagged jets to either of the visible frames at an approximately equal frequency, while for compressed SUSY signal events whose topology is in agreement with that of the ISR decay tree imposed, a more accurate assignment of objects is achieved. A requirement of at least two c-tagged jets in the S frame is imposed for the CA, CB and CC signal regions, and exactly one for SR1.

Reinterpretation for DM

$$\mathcal{L}_{\mathrm{RH}} \supset \lambda_{\mathrm{ij}} \bar{u_{\mathrm{Ri}}} \chi_{\mathrm{j}} \phi + \mathrm{h.c}$$

$$\mathcal{L}_{\mathrm{LH}} \supset \lambda_{\mathrm{ij}} \bar{u_{\mathrm{Li}}} \chi_{\mathrm{j}} \phi_{\mathrm{u}} + \tilde{\lambda}_{\mathrm{ij}} \bar{d_{\mathrm{Li}}} \chi_{\mathrm{j}} \phi_{\mathrm{d}} + \mathrm{h.c}$$

in $t\bar{t}$ events (Figure 1(c)). At low $D_{\lambda,11}$ values, the s-channel dominates over the other two production modes, representing around 100% of the total cross-section at $D_{\lambda,11} \approx 0$, while at values close to 2.0, it represents less than 10% of the total cross-section and the other diagrams dominate.

Table 2: Percentage of events in tc+DM (tt+DM) final states for some representative signal points of the four benchmark models in Table 1.

RH-SFF	$D_{\lambda,11} = 0.25$	$D_{\lambda,11} = 1.0$	$D_{\lambda,11} = 1.75$
m_ϕ = 400 GeV	8%(71%)	28%(39%)	34%(30%)
m_ϕ = 800 GeV	4%(86%)	18%(61%)	24%(50%)
m_ϕ = 1200 GeV	9% (87%)	17%(63%)	23%(52%)
RH-QDF	$D_{\lambda,11} = 0.25$	$D_{\lambda,11} = 1.0$	$D_{\lambda,11} = 1.75$
m_ϕ = 400 GeV	27%(46%)	26%(28%)	37%(25%)
m_ϕ = 800 GeV	20%(57%)	30%(39%)	32%(36%)
m_ϕ = 1200 GeV	20%(59%)	30%(40%)	31%(37%)
LH-QDF1	$D_{\lambda,11} = 0.25$	$D_{\lambda,11} = 1.0$	$D_{\lambda,11} = 1.75$
m_ϕ = 400 GeV	33%(35%)	38%(25%)	38%(23%)
m_ϕ = 800 GeV	27%(47%)	32%(35%)	33%(33%)
m_ϕ = 1200 GeV	25%(47%)	31%(35%)	32%(34%)
LH-QDF2	$D_{\lambda,11} = 1.0$	$D_{\lambda,11} = 1.5$	$D_{\lambda,11} = 2.0$
m_ϕ = 600 GeV	51%(0%)	51%(0%)	51%(0%)
m_ϕ = 900 GeV	31%(38%)	32%(35%)	33%(34%)
m_ϕ = 1400 GeV	28%(39%)	30%(37%)	31%(35%)

Reinterpretation for DM

RH benchmarks

Exclusion limits reach up to 1.2 TeV for, or up to ~ 800 GeV for $D_{\lambda,11} \sim 1$

For RH-QDF, $m_\phi = 400$ GeV and $D_{\lambda,11} \approx 0.25$ could be excluded

LH-QDF1

Exclusion limits reach up to 1.2 TeV for $D_{\lambda,11} \approx 2$, or up to 600 GeV for $D_{\lambda,11} \approx 1.1$

Exclusion limits around 400. GeV for $D_{\lambda,11} \approx 0$

LH-QDF2

Smaller limit due to larger m_χ

Signal models with $m_\phi \in [750{,}1100]$ GeV and $D_{\lambda,11} > 1.75$ can be excluded